

### Clinical and radiological characterization of fibrous hamartoma of infancy

Dear Editor,

A newborn male patient presented with suspected obstetric trauma due to increased forearm diameter. An X-ray of the forearm (Figure 1A) showed fracture of the ulna and bowing of the radius, together with increased thickness and density of the adjacent soft tissues. Intravenous contrast-enhanced magnetic resonance imaging (Figures 1B, 1C, and 1D) revealed a heterogeneous, infiltrative tissue formation, with ill-defined and therefore difficult to measure borders, the epicenter of which was in the interosseous membrane of the middle and distal thirds of the forearm. The formation was infiltrating the muscle planes on the volar and dorsal faces of the forearm and was in contact with the vascular-nervous bundles, although there were no signs that it had invaded the bundles. The lesion created discontinuity in the middle third of the ulna and the bowing of the radius. Heterogeneous contrast enhancement was observed, as were lipid material from the lesion and fibrotic streaks.

An incisional biopsy was performed. Histological and immunohistochemical analysis of the biopsy specimen demonstrated positivity for vimentin alpha-actin and for S-100 protein, together with negativity for desmin. On the basis of those findings, the definitive diagnosis of fibrous hamartoma of infancy (FHI) was made.

A benign soft-tissue tumor that typically occurs in the first two years of life<sup>(1)</sup>, FHI was first described in 1956 by Reye<sup>(2)</sup>, who dubbed it subdermal fibromatous tumor of infancy. There have been fewer than 200 cases reported to date, only 8 having been reported in the literature of Latin America; 91% of all cases occurred in the first year of life, 25% having been diagnosed at birth<sup>(3)</sup>.

The differential diagnosis of FHI includes all other soft-tissue tumors. When the tumor is hard and fixed to the deep planes, it is important not to confuse FHI with malignant neoplasms such as juvenile fibromatosis and sarcoma (especially rhabdomyosarcoma and fibrosarcoma, which typically affect young children). Neural tumors (mainly neurofibromas) and vascular tumors should also be excluded<sup>(4,5)</sup>. The identification of fat within the lesion helps narrow down the differential diagnosis, as do patient age and form of presentation. In the appropriate clinical context, a finding of fibrous tissue trabeculae interspersed with fat in an organized pattern is strongly suggestive of FHI<sup>(6)</sup>.

The occurrence of FHI is not related to syndromes or a positive family history<sup>(5)</sup>. Larger lesions typically involve neurovascular structures. Although the tumors are infiltrative, with ill-defined borders and no capsule, they typically do not invade the surrounding bone structures<sup>(5)</sup>.

Reportedly, FHI is painless and its growth is unpredictable. It can grow rapidly in early childhood, its rate of growth slowing after the child has reached five years of age. There have been no reports of spontaneous involution or malignancy<sup>(3)</sup>.

Histopathological examination of an FHI shows compounds of mature adipose tissue interspersed with bands of dense fibrous tissue rich in myofibroblasts and collagen<sup>(5)</sup>. Together with the bands of connective tissue, an FHI presents nests of primitive mesenchyma represented by small, rounded, immature cells, without areas of atypia but occasionally with mitoses, immersed in a myxoid matrix, possibly constituting an anomalous process of tissue maturation.

The preferred treatment for FHI is complete local resection<sup>(6)</sup>, no adjunctive therapies being required. Recurrence after

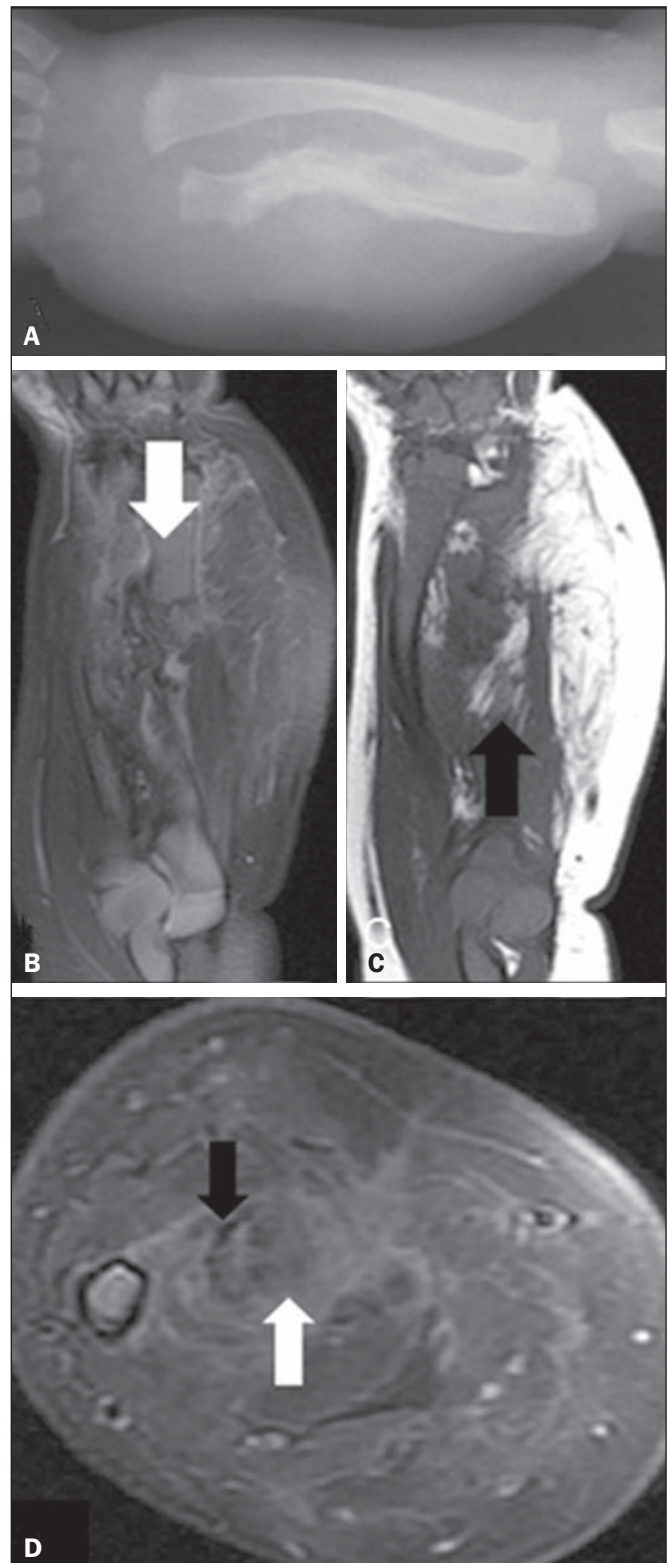


**Figure 1.** **A:** Forearm X-ray showing fracture associated with ulna irregularity and bowing of the radius, together with increased thickness and density of the soft parts of the forearm. **B:** Fat-saturated, T2-weighted magnetic resonance imaging scan, in the coronal plane, showing discontinuity of the ulna (arrow), the full extent of the lesion, and suppression of the fatty content. **C:** T1-weighted magnetic resonance imaging scan, in the coronal plane, highlighting the lipid content of the lesion (arrow). **D:** Proton-density axial magnetic resonance imaging slice in the region of the fractured ulna showing the contrast uptake by the dense fibrous stroma, the fibrotic streaks (black arrow), and the suppressed signaling of the fat content (white arrow).

complete resection is uncommon, having been reported in only approximately 10% of cases<sup>(5)</sup>.

REFERENCES

1. Saab ST, McClain CM, Coffin CM. Fibrous hamartoma of infancy: a clinicopathologic analysis of 60 cases. *Am J Surg Pathol.* 2014;38:394–401.
2. Reye RD. A consideration of certain subdermal fibromatous tumours of infancy. *J Pathol Bacteriol.* 1956;72:149–54.
3. Dickey GE, Sotelo-Avila C. Fibrous hamartoma of infancy: current review. *Pediatr Dev Pathol.* 1999;2:236–43.
4. Eich GF, Hoeffel JC, Tschäppeler H, et al. Fibrous tumours in children: imaging features of a heterogeneous group of disorders. *Pediatr Radiol.* 1998;28:500–9.
5. Jesus LE, Gameiro VS, Novelli RJ, et al. Hamartoma fibroso infantil:

lesão volumosa com envolvimento de plexo braquial. *Acta Ortop Bras.* 2006;14:229–30.

6. Laffan EE, Ngan BY, Navarro OM. Pediatric soft-tissue tumors and pseudotumors: MR imaging features with pathologic correlation: part 2. Tumors of fibroblastic/myofibroblastic, so-called fibrohistiocytic, muscular, lymphomatous, neurogenic, hair matrix, and uncertain origin. *Radiographics.* 2009;29:e36.

**Vagner Moysés Vilela<sup>1</sup>, Valéria Mota Ribeiro<sup>1</sup>, Jairo Campos Paiva<sup>1</sup>, Diego Demolinari Pires<sup>1</sup>, Lucas Scodeler Santos<sup>1</sup>**

1. Universidade Federal de Juiz de Fora (UFJF), Juiz de Fora, MG, Brazil. Mailing address: Dr. Lucas Scodeler Santos. Rua Marquês de Itu, 679, ap. 24, Vila Buarque. São Paulo, SP, Brazil, 01223-000. E-mail: lucasscodeler@yahoo.com.br.

<http://dx.doi.org/10.1590/0100-3984.2015.0085>

**Left renal vein thrombosis secondary to compression by the uncinate process of the pancreas, mimicking the nutcracker syndrome**

Dear Editor,

A 40-year-old woman presented with a five-month history of pain in a portion of the mesogastrium and in the left side. She reported recent weight loss (of 5 kg) after having had dengue fever. She also reported no comorbidities and stated that she was not using contraceptives. The physical examination revealed Giordano’s sign on the left side. The results of the blood count and urinalysis were normal. Computerized tomography of the abdomen showed compression of the left renal vein (LRV) caused by the uncinate process of the pancreas pressing against the aorta,

leading to dilation of the proximal segment, with an intraluminal thrombus (Figures 1A and 1B), dilation of the collateral perirenal venous system, dilation of the gonadal veins, and ipsilateral pelvic varices (Figures 1C and 1D). The patient was treated with oral anticoagulants for four months and declined to have a stent placed in the LRV.

Vascular compressive syndromes occur in less than 1% of the cases and represent vascular trapping between rigid surfaces, which lead to manifestations caused by hypertension, venous congestion, thrombosis, and arterial ischemia<sup>(1–4)</sup>.

The causes of compression of the LRV include expansive retroperitoneal formations, anatomical variations, and nutcracker syndrome (NCS)<sup>(2)</sup>. NCS is usually caused by the trapping of the LRV between the superior mesenteric artery and the abdominal

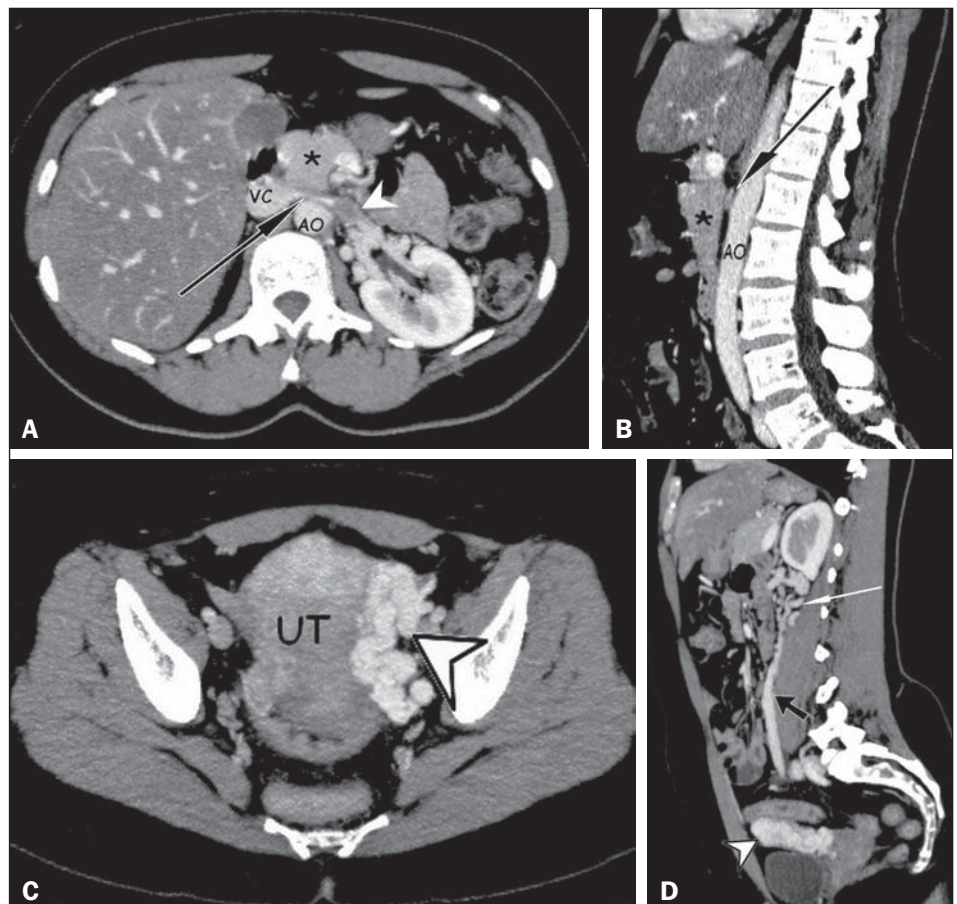


**Figure 1. A,B:** Contrast-enhanced arterial-phase CT of the abdomen, in the axial plane and in sagittal reconstruction, respectively, characterizing clots within the proximal portion of the LRV (white arrowhead), showing a reduction in its caliber at the aortomesenteric compression (black arrows), close to its junction with the inferior vena cava (VC), due to the extrinsic compression exerted by the uncinate process of the pancreas (asterisks) against the aorta (AO). Additional finding: diffuse hypointense signal in the hepatic parenchyma, suggesting fatty infiltration. **C,D:** Contrast-enhanced arterial-phase CT of the abdomen, in the axial plane and in sagittal reconstruction, respectively, showing dilation of the pelvic vessels (arrowheads) near the left lateral aspect of the uterus and the left gonadal vein (black arrow), with dilated collateral veins in the ipsilateral perirenal space (white arrow).